*Stanford Exploration Project, Report 95, October 10, 1997, pages 77–100*

# Time-domain anisotropic processing in arbitrarily inhomogeneous media

*Tariq Alkhalifah, Sergey Fomel, and Biondo Biondi*[1]

***keywords:*** *traveltime, modeling, anisotropy*


## ABSTRACT

In transversely isotropic media with a vertical axis of symmetry (VTI media), we can represent the image in vertical time, as opposed to depth, thus eliminating the inherent ambiguity of resolving the vertical $P$-wave velocity from surface seismic data. In this new $(x-\tau)$-domain, the raytracing and eikonal equations are completely independent of the vertical $P$-wave velocity, on the condition that the ratio of the vertical to normal-moveout (NMO) $P$-wave velocity ($\alpha$) is laterally invariant. Practical size departures of $\alpha$ from lateral homogeneity affect traveltimes only slightly. As a result, for all practical purposes, the VTI equations in the $(x-\tau)$-domain become dependent on only two parameters in laterally inhomogeneous media: the NMO velocity for a horizontal reflector, and an anisotropy parameter, $\eta$. An acoustic wave equation in the $(x-\tau)$-domain is also independent of the vertical velocity. It includes an unsymmetric Laplacian operator to accommodate the unbalanced axis units in this new domain. In summary, we have established the basis for a full inhomogeneous time-processing scheme in VTI media that is dependent on only $v$ and $\eta$, and independent of the vertical $P$-wave velocity.


## INTRODUCTION

The main feature of the anisotropic parameter representation suggested by Alkhalifah and Tsvankin (1995) is that time processing—normal moveout correction (NMO), dip moveout (DMO), and time migration-become independent of vertical $P$—wave velocity, a parameter necessary to resolve reflector depth. As a result, estimating the vertical velocity is unnecessary for time processing, which depends on only two parameters: the normal-moveout (NMO) velocity for a horizontal reflector and an anisotropy parameter denoted by $\eta$. However, this rather fortunate behavior of seismic waves in transversely isotropic media with a vertical symmetry axis (VTI media)

[1]**email:** tariq@sep.stanford.edu, sergey@sep.stanford.edu, biondo@sep.stanford.edu

seems to hold only for vertically inhomogeneous media. When lateral inhomogeneity exists, three parameters are needed to characterize the medium and implement processing.

Our goal is to implement time processing that truly honors the lateral inhomogeneity of the medium, and yet is independent of the vertical $P$-wave velocity. Separating the $P$-wave vertical velocity, $v_v$, from the image processing stage helps in avoiding the intrinsic ambiguity that this velocity introduces into the problem of estimating parameters in VTI models. This separation allows us to correct for the depth whenever such information becomes available, for example, well-log data.

This report shows that certain lateral inhomogeneities fall into this fortunate category of independence from vertical $P$-wave velocity when we replace the depth axis with the vertical time. We refer to such an inhomogeneity as being *factorized laterally*. The term *factorized* was introduced by Shearer and Chapman (1988) to describe a medium in which the ratio between the different elastic coefficients remains constant throughout the medium. In the case of our new coordinate system, this constraint is needed only between the NMO velocity and vertical velocity and it is needed only laterally. In other words, $\alpha$, defined as the ratio between the vertical and NMO $P$-wave velocity, can change only vertically. This condition still allows for data processing in media of any lateral inhomogeneity, but does not allow for applying any depth conversion. In fact, this condition is extremely convenient considering that reflector depth is typically resolved at only one location along a given seismic line (at the well), and that we can therefore use this $\alpha(z)$, extracted from the well, to estimate depths. When $\alpha$ varies laterally, the accuracy of the processing depends on the size of the variation. Our analysis shows that such dependency is small for typical variations and, as a result, can be ignored.

The term *time processing* implies that an image of the subsurface is obtained with its vertical axis given in time rather than in depth. Traditionally, only vertical inhomogeneity was treated in the processing of this image. Such processing might include approximations to treat mild inhomogeneities, but nothing that could come close to properly imaging complex data such as the Marmousi model. *Time processing* takes on a quite different meaning in this paper. It includes exact treatment for media with any lateral inhomogeneity. Specifically, we develop ray-theoretical solutions of wave propagation in the time domain, including the eikonal and raytracing equations that can handle any lateral inhomogeneity. An acoustic wave equation constrains all other aspects (such as amplitudes) of wave propagation in the $(x-\tau)$-domain.

We also show numerical results of raytracing and examine its dependence on only two parameters in VTI media.

## PARAMETERIZATION IN ANISOTROPIC MEDIA

In homogeneous transversely isotropic media with a vertical symmetry axis (VTI media), *P*- and *SV*-waves [2] can be described by the vertical velocities $V_{P0}$ and $V_{S0}$ of *P*- and *S*-waves, respectively, and two dimensionless parameters $\epsilon$ and $\delta$ (Thomsen, 1986). Tsvankin and Thomsen (1994) and Alkhalifah (1997) demonstrated that *P*-wave velocity and traveltime are practically independent of $V_{S0}$, even for strong anisotropy. Thus, for practical purposes, *P*-wave kinematic signatures can be considered a function of just three parameters: $V_{P0}$, $\delta$, and $\epsilon$.

Alkhalifah and Tsvankin (1995) further demonstrated that a new representation in terms of just two parameters is sufficient for performing all time-related processing, such as normal moveout correction (including nonhyperbolic moveout correction, if necessary), dip-moveout removal, and prestack and post-stack time migration, assuming that the velocity varies only vertically. These two parameters are the normal-moveout velocity for a horizontal reflector

$$V_{\rm nmo}(0) = V_{p0}\sqrt{1+2\delta}\,, \tag{1}$$

and the anisotropy coefficient

$$\eta \equiv 0.5\left(\frac{V_h^2}{V_{\rm nmo}^2(0)} - 1\right) = \frac{\epsilon-\delta}{1+2\delta}\,, \tag{2}$$

where $V_h$ is the horizontal velocity. Instead of $V_{\rm nmo}$, we use $v$ to denote the interval NMO velocity in both isotropic and TI media.

## THE DEPTH ISSUE

The depth axis has always been a source of uncertainty in seismic processing. Geophysicist have shied away from predicting depths from surface seismic *P*-wave data. Typically, well-log data are used for such a task. However, since well-log data are rare and sparse, seismically based interpolation of well-log information is commonly used. Although the conventional isotropic theory suggests that depth can be resolved using the velocity field that focuses the seismic image, field data have rarely agreed with this isotropic principal. Anisotropy, on the other hand, suggests that depth cannot be resolved using surface seismic data. The velocity needed to resolve depth is the vertical velocity, which is different from the imaging velocity (the velocity that yields the best image). This difference accords with the typical field data experience. In fact, in VTI media, processing is controlled by three velocities: one responsible for depth mapping, another for stacking, and the third for migration. Although this is a simplistic representation and theory suggests that there is more interaction between these velocities and their influences, such a representation is close to what actually

[2] We omit the qualifiers in *quasi-P-wave* and *quasi-SV-wave* for brevity.

happens in practice. Two of these velocities are resolvable from surface seismic data, or, in a general inhomogeneous case, two combinations of these velocities are resolvable, which implies the existence of a null space in the three-parameter representation of VTI media.

Considering that depth in VTI media is determined by multiplying half of the vertical traveltime with the vertical velocity, it seems that representing data with the vertical time, instead of depth, could absorb the vertical velocity influence. This has been shown to be the case for vertically inhomogeneous media (Alkhalifah and Tsvankin, 1995) but has yet to be shown for more general inhomogeneity. In the next section, we replace the depth axis with vertical time to represent more general, arbitrarily inhomogeneous media.

## REPRESENTING DEPTH WITH VERTICAL TIME

In this section, we derive the relation between the depth and vertical time axis for a general inhomogeneous medium. Using this relation, the VTI eikonal equation is represented in the new $(x-\tau)$-domain coordinate system. We have derived a similar relation in another paper (Biondo et al., 1997); for isotropic media. Also Hatton et al. (1981) implemented a similar mapping to show the limitations of time migration.

Two-way vertical time is related to depth by the following relation,

$$\tau(x,z) = \int_0^z \frac{2}{v_v(x,\zeta)} d\zeta, \tag{3}$$

where $v_v$ is the vertical $P$-wave velocity, which can vary vertically as well as laterally. As follows from equation 3, the stretch applied to the depth axis is laterally variant.

Alkhalifah (1997d) derived a simple form of the eikonal equation for VTI media, based on setting the shear wave velocity to zero. For 2-D media, it is

$$v^2\ (1+2\,\eta)\ \left(\frac{\partial t}{\partial x}\right)^2 - {v_v}^2 \left(\frac{\partial t}{\partial z}\right)^2\ \left(1-2\,v^2\,\eta\left(\frac{\partial t}{\partial x}\right)^2\right) = 1. \tag{4}$$

This equation, based on the acoustic medium assumption in VTI media, though not physically possible, yields extremely accurate traveltime solutions that are close to what we get for typical elastic media.

The eikonal equation includes first-order derivatives of traveltime with respect to position. In order to transform this eikonal equation from the depth to the time coordinate, we need to replace $x$ with $\tilde{x}$. Using the chain rule, $\frac{\partial t}{\partial x}$ in the eikonal equation 4 is given by

$$\frac{\partial t}{\partial x} = \frac{\partial t}{\partial \tilde{x}} + \frac{\partial t}{\partial \tau}\sigma, \tag{5}$$

where $\sigma$, extracted from equation (3), is written as

$$\sigma(x,z) = \frac{\partial \tau}{\partial x} = \int_0^z \frac{\partial}{\partial x}\left(\frac{1}{v_v(x,\zeta)}\right)\ d\zeta. \tag{6}$$

Likewise, the partial derivative in $z$ in the eikonal equation is

$$\frac{\partial t}{\partial z} = \frac{2}{v_v}\frac{\partial t}{\partial \tau}. \tag{7}$$

Therefore, the transformation from $(x,\ z)$ to $(\tilde{x},\ \tau)$ is governed by the following Jacobian matrix in 2-D media:

$$J = \begin{pmatrix} 1 & \sigma \\ 0 & \frac{2}{v_v} \end{pmatrix} \tag{8}$$

Substituting equations (5) and (7) into the eikonal equation (4) yields the equation

$$v^2\ (1+2\,\eta)\left(\frac{\partial t}{\partial \tilde{x}} + \frac{\partial t}{\partial \tau}\sigma\right)^2 - 4\left(\frac{\partial t}{\partial \tau}\right)^2\left(1 - 2\,v^2\,\eta\left(\frac{\partial t}{\partial \tilde{x}} + \frac{\partial t}{\partial \tau}\sigma\right)^2\right) = 1, \tag{9}$$

which is indirectly independent of the vertical velocity. However, according to equation (6), $\sigma$ still depends on the vertical $P$-wave velocity. Rewriting equation (6) in terms of the two-way vertical time (see Appendix A) gives us

$$\sigma(\tilde{x},\tau) = \frac{-1}{v_v(\tilde{x},\tau)}\int_0^\tau \frac{\partial v_v(\tilde{x},\tilde{\tau})}{\partial \tilde{x}}\ d\tilde{\tau}, \tag{10}$$

where $\tilde{x}$ corresponds to the new coordinates $(\tilde{x},\tau)$. In the case of $v_v(x,z) = \alpha(z)v(x,z)$, which is a special case of lateral inhomogeneity, referred to here as *laterally factorized*, equation (6) takes the form

$$\sigma(x,\tau) = \int_0^\tau \frac{\partial}{\partial x}\left(\frac{1}{v}\right)\ v d\tilde{\tau}, \tag{11}$$

which is clearly independent of the vertical $P$-wave velocity. Also, equation (10) becomes

$$\sigma(\tilde{x},\tau) = \frac{-1}{v(\tilde{x},\tau)}\int_0^\tau \frac{\partial v(\tilde{x},\tilde{\tau})}{\partial \tilde{x}}\ d\tilde{\tau}. \tag{12}$$

The eikonal equation can be used to compute seismic traveltimes in laterally factorized inhomogeneous media without the need to estimate the vertical $P$-wave velocity. The departure of the medium from this special condition of laterally factorized media will cause errors in traveltime calculation. We can estimate these errors by evaluating how much $\sigma$ varies between equations (6) and (11). Specifically, if $v_v(x,z) = \alpha(x,z)v(x,z)$ then

$$\Delta\sigma(x,\tau) = \int_0^\tau \frac{\partial}{\partial x}\left(\frac{1}{\alpha}\right)\ d\tilde{\tau}. \tag{13}$$

If the ratio of the vertical to NMO velocity, $\alpha$, does not change laterally, $\Delta\sigma$ is equal to zero, and thus no errors will occur in traveltime calculation. The departure of $\sigma$ from zero affects only the $x$ axis component of the wavefront; according to equations (5) and (7) it is only $\frac{\partial t}{\partial x}$ that depends on $\sigma$. The vertical component of the traveltime remains accurate no matter how much $\alpha$ varies laterally. Also, because the eikonal equation is independent of $\sigma$ for vertically traveling waves ($\frac{\partial t}{\partial \tau}$=0), such waves are

error-free. The majority of the errors caused by lateral $\alpha$ variation occurs around 45-degree wave propagation.

In terms of VTI parameters, the NMO velocity is given by (Thomsen, 1986)

$$v(x,z) = v_v(x,z)\sqrt{1+2\delta(x,z)}.$$

Therefore,

$$\alpha(x,z) = \frac{1}{\sqrt{1+2\delta(x,z)}},$$

and

$$\frac{d\alpha}{dx} = -\frac{1}{(1+2\delta(x,z))^{\frac{3}{2}}}\frac{d\delta}{dx} \approx -\frac{d\delta}{dx}.$$

Then

$$\Delta\sigma = -2\int_0^\tau \frac{d\delta}{dx}d\tilde{\tau}.$$

We can see that the absolute error, resulting from the integral formulation, clearly increases with time.

In addition, when we use the new coordinate system $(x,\tau)$, the transport equation becomes independent of the vertical velocity under the same condition of laterally factorized media (see Appendix B). Bellow, and for simplicity, we will replace $\tilde{x}$ with $x$ to denote the lateral coordinate in the new coordinate system.

## RAYTRACING EQUATIONS

Using the method of characteristics, we can derive a system of ordinary differential equations that define the ray trajectories. To do so, we need to transform equation (9) to the following form:

$$F\left(x,\tau,\frac{\partial t}{\partial x},\frac{\partial t}{\partial \tau}\right) = 0, \tag{14}$$

or

$$F\left(x,\tau,p_x,p_\tau\right) = 0, \tag{15}$$

where $p_x = \frac{\partial t}{\partial x}$ and $p_\tau = \frac{\partial t}{\partial \tau}$. According to the classic rules of mathematical physics (Courant, 1966), the solutions of this kinematic equation can be obtained from the system of ordinary differential equations

$$\begin{aligned} \frac{dx}{ds} &= \frac{1}{2}\frac{\partial F}{\partial p_x} \quad , \quad \frac{d\tau}{ds} = \frac{1}{2}\frac{\partial F}{\partial p_\tau}, \\ \frac{dp_x}{ds} &= -\frac{1}{2}\frac{\partial F}{\partial x} \quad , \quad \frac{dp_\tau}{ds} = -\frac{1}{2}\frac{\partial F}{\partial \tau}, \end{aligned} \tag{16}$$

where $s$ is a running parameter along the rays, related to the traveltime $t$ as follows:

$$\frac{dt}{ds} = \frac{1}{2}p_\tau\frac{\partial F}{\partial p_\tau} + p_x\frac{\partial F}{\partial p_x},$$

with

$$\frac{dx}{dt} = \frac{dx}{ds}\Big/\frac{dt}{ds} \quad , \qquad \frac{d\tau}{dt} = \frac{d\tau}{ds}\Big/\frac{dt}{ds} \, ,$$
$$\frac{dp_x}{dt} = \frac{dp_x}{ds}\Big/\frac{dt}{ds} \quad , \qquad \frac{dp_\tau}{dt} = \frac{dp_\tau}{ds}\Big/\frac{dt}{ds} \, . \tag{17}$$

Using equation (9), we obtain

$$\frac{dx}{ds} = a\, v^2 \, \left(1 + 2\,\eta \, \left(1 - 4\, {p_\tau}^2\right)\right), \tag{18}$$

$$\frac{d\tau}{ds} = 4\, p_\tau - a\, v^2 \, \left(-\sigma + 2\,\eta \, \left(-\sigma + 4\, p_x\, p_\tau + 8\, \sigma\, {p_\tau}^2\right)\right), \tag{19}$$

$$\frac{dp_x}{ds} = -a^2\, v \, \left(1 + 2\,\eta \, \left(1 - 4\, {p_\tau}^2\right)\right) \, v_x$$
$$-a\, v^2 \, \left(a \, \left(1 - 4\, {p_\tau}^2\right) \, \eta_x + p_\tau \, \left(1 + 2\,\eta - 8\,\eta\, {p_\tau}^2\right) \, \sigma_x\right), \tag{20}$$

$$\frac{dp_\tau}{ds} = -v\, a^2 \, \left(1 + 2\,\eta \, \left(1 - 4\, {p_\tau}^2\right)\right) \, v_\tau$$
$$-v^2\, a \, \left(a \, \left(1 - 4\, {p_\tau}^2\right) \, \eta_\tau + p_\tau \, \left(1 + 2\,\eta - 8\,\eta\, {p_\tau}^2\right) \, \sigma_\tau\right), \tag{21}$$

and

$$\frac{dt}{ds} = 4\, {p_\tau}^2 + a^2\, v^2 \, \left(1 + 2\,\eta \, \left(1 - 8\, {p_\tau}^2\right)\right),$$

where

$$a = p_x + \sigma\, p_\tau,$$

and $v_x = \frac{\partial v}{\partial x}$ and $v_\tau = \frac{\partial v}{\partial \tau}$, and the same holds for $\eta$ and $\sigma$.

To trace rays, we must first identify the initial values $x_0$, $\tau_0$, $p_{x0}$, and $p_{\tau 0}$. The variables $x_0$ and $\tau_0$ describe the source position, and $p_{x0}$ and $p_{\tau 0}$ are extracted from the initial angle of propagation. Note that, from equation (9),

$$p_{\tau 0} = 1 - \frac{v^2 p_{x0}^2}{1 - 2\eta v^2 p_{x0}^2},$$

because $\sigma$=0 at the source position ($z$=0).

The raytracing system of equations (18-21) describes the ray-theoretical aspect of wave propagation in the $(x-\tau)$-domain, and can be used as an alternative to the eikonal equation. Numerical solutions of the raytracing equations, as opposed to the eikonal equation, provide multi-arrival traveltimes and amplitudes. In the numerical examples, we use raytracing to highlight some of the features of the $(x-\tau)$-domain coordinate system.

## THE $X-TAU$ ACOUSTIC WAVE EQUATION

Following the approach of Alkhalifah (1997d), an acoustic wave equation is simply derived from the eikonal equation using Fourier transformations. The addition of $\sigma$ results in a more intriguing wave equation than the one derived by Alkhalifah. Instead of the symmetric form of the familiar Laplacian in isotropic media, two sources of unsymmetry are introduced into the new wave equation. One is caused by the unbalanced new coordinate system with one axis given in time and the other in position. The second, caused by anisotropy, is similar to that which Alkhalifah described.

Using $k_x = \omega\frac{\partial t}{\partial x}$, and $k_\tau = \omega\frac{\partial t}{\partial \tau}$, where $k_x$ is the horizontal component of the wavenumber vector, $k_\tau$ is the vertical-time-normalized component of the wavenumber vector, and $\omega$ is the angular frequency, we can transform equation (9) to

$$v^2\ (1+2\,\eta)\left(\frac{k_x}{\omega}+\frac{k_\tau}{\omega}\sigma\right)^2-4\left(\frac{k_\tau}{\omega}\right)^2\left(1-2\,v^2\,\eta\left(\frac{k_x}{\omega}+\frac{k_\tau}{\omega}\sigma\right)^2\right)=1. \tag{22}$$

Multiplying both sides of equation (22) with the wavefield in the Fourier domain, $F(k_x,k_\tau,\omega)$, as well as using inverse Fourier transform on $k_\tau$, $k_x$ and $\omega$ ($k_\tau \rightarrow -i\frac{d}{d\tau}$, $k_x \rightarrow -i\frac{\partial}{\partial x}$, and $\omega \rightarrow i\frac{\partial}{\partial t}$), we obtain the acoustic wave equation in this new vertical-velocity-independent coordinate system,

$$\begin{aligned}\frac{\partial^4 F}{\partial t^4} = -8\,\frac{\partial^4 F}{\partial x^2\partial\tau^2}\,v^2\,\eta \;&+\; \frac{\partial^4 F}{\partial x^2\partial t^2}\,v^2\ (1+2\,\eta)-16\,\frac{\partial^4 F}{\partial x\partial\tau^3}\,v^2\,\eta\,\sigma+2\,\frac{\partial^4 F}{\partial t^2\partial x\partial\tau}\,v^2\ (1+2\,\eta)\,\sigma\\ &-\; 8\,\frac{\partial^4 F}{\partial\tau^4}\,v^2\,\eta\,\sigma^2+\frac{\partial^4 F}{\partial t^2\partial\tau^2}\left(4+v^2\ (1+2\,\eta)\,\sigma^2\right).\end{aligned} \tag{23}$$

This equation is a fourth-order partial differential equation. Unlike, the acoustic wave equation for VTI media of Alkhalifah (1997d), equation (23) has odd-order derivatives caused by the unsymmetry of the coordinate system. Setting $\sigma = 0$ [$v(z)$=0], we obtain a similar equation, with $\partial z$ replaced by $v_v\partial\tau$ as follows:

$$\frac{\partial^4 F}{\partial t^4} = -8\,\frac{\partial^4 F}{\partial x^2\partial\tau^2}\,v^2\,\eta+\frac{\partial^4 F}{\partial x^2\partial t^2}\,v^2\ (1+2\,\eta)+4\frac{\partial^4 F}{\partial t^2\partial\tau^2}. \tag{24}$$

Setting $\eta = 0$ in equation (23) yields the acoustic equation for elliptically anisotropic media:

$$\frac{\partial^2}{\partial t^2}\left(\frac{\partial^2 F}{\partial t^2}-v^2\left(\frac{\partial^2 F}{\partial x^2}+2\,\frac{\partial^2 F}{\partial x\partial\tau}\,\sigma\right)-\frac{\partial^2 F}{\partial\tau^2}\left(4+v^2\,\sigma^2\right)\right)=0. \tag{25}$$

Substituting $P = \frac{\partial^2 F}{\partial t^2}$, we obtain the second-order wave equation for elliptically anisotropic media:

$$\frac{\partial^2 P}{\partial t^2} = v^2\left(\frac{\partial^2 P}{\partial x^2}+2\,\frac{\partial^2 P}{\partial x\partial\tau}\,\sigma\right)+\frac{\partial^2 P}{\partial\tau^2}\left(4+v^2\,\sigma^2\right). \tag{26}$$

Rewriting equation (23) in terms of $P(x,y,z,t)$ rather than $F(x,y,z,t)$, wherever possible, yields

$$\frac{\partial^2 P}{\partial t^2} = -8\,\frac{\partial^4 F}{\partial x^2 \partial \tau^2}\,v^2\,\eta + \frac{\partial^2 P}{\partial x^2}\,v^2\,(1+2\,\eta) - 16\,\frac{\partial^4 F}{\partial x \partial \tau^3}\,v^2\,\eta\,\sigma + 2\,\frac{\partial^2 P}{\partial x \partial \tau}\,v^2\,(1+2\,\eta)\,\sigma$$
$$-8\,\frac{\partial^4 F}{\partial \tau^4}\,v^2\,\eta\,\sigma^2 + \frac{\partial^2 P}{\partial \tau^2}\,\left(4 + v^2\,(1+2\,\eta)\,\sigma^2\right), \quad (27)$$

where

$$F(x,y,z,t) = \int_0^t dt' \int_0^{t'} P(x,y,z,\tau) d\tau.$$

Because of its second-order nature in time, equation (27) is simpler to use in a numerical implementation than equation (23). The acoustic wave equation in $(x-\tau)$-domain is clearly independent of the vertical velocity when $\sigma$ is given by equation 12 and $\alpha$ is laterally invariant.

## NUMERICAL EXAMPLES

Using the ray-tracing system of equations derived earlier, we can compute traveltimes numerically. Unlike numerical solutions of the eikonal equation, raytracing provides multi-arrival traveltimes and amplitudes. We want to confirm numerically the following two aspects of implementing raytracing in the new coordinate system:

- The traveltime solution when transformed to depth agrees with results from conventional depth-domain raytracing.
- The traveltime solution in the $(x-\tau)$-domain is independent of the vertical $P$-wave velocity for media that are factorized laterally $[\alpha(z)]$.

Figure 1 shows sixteen rays originating from a source on the surface at position $x = 0$ through the same depth velocity model of $v_v(x,z) = 1.5 + 0.225z + 0.15x$, $v(x,z) = 2.0 + 0.3z + 0.2x$, and $\eta(x,z) = 0.1 + 0.05z + 0.05x$ using conventional raytracing in the depth domain (black curves), and the new raytracing in the $(x-\tau)$-domain (gray curve). We achieved the $(x-\tau)$-domain ray tracing results by mapping the depth velocity model to time using equation (3), and then mapping the ray solutions back to depth using equation (D-2). The sixteen rays have ray parameters ranging from zero to the maximum value of $1/V_h$ ($V_h$ is the horizontal velocity), with a fixed ray-parameter spacing of $1/(15V_h)$. The rays terminate at the same time of 8 s, and the wavefronts (given by the dashed curves) are plotted at about 1.6-s intervals. The wavefronts that correspond to the different raytracings are virtually coincident, a result that agrees with our analytical findings.

In Figure 2, we check for another aspect of the theory, that is, the independence of raytracing from the vertical velocity for laterally factorized VTI media. Again,

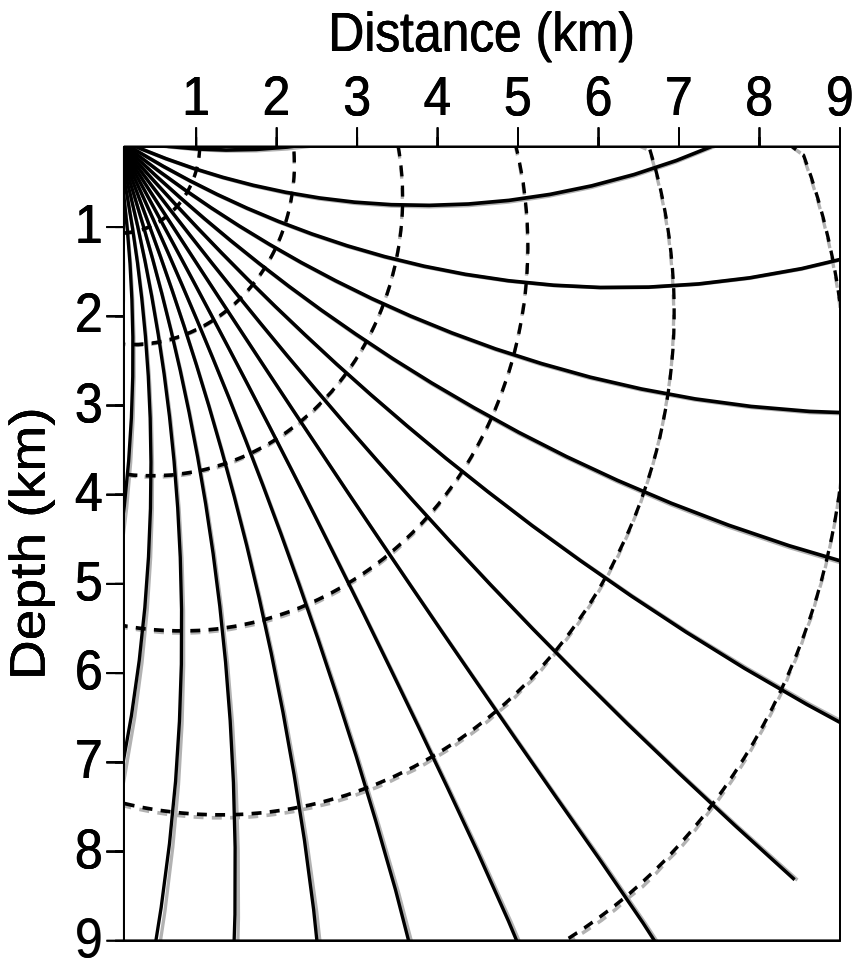


Figure 1: Raypaths (solid curves) and corresponding wavefronts (dashed curves) for an inhomogeneous VTI model with $v(x,z) = 2.0 + 0.3z + 0.2x$ km/s, $v_v(x,z) = 1.5 + 0.225z + 0.15x$ km/s, and $\eta(x,z) = 0.1 + 0.05z + 0.05x$. The black curves are obtained through conventional raytracing in the depth domain, and the gray curves are obtained using the equivalent $(x-\tau)$-domain raytracing, where the results are ultimately converted to depth. In this case, the curves nearly overlap; they are only barely distinguishable, which agrees with the theoretical results. The small difference is numerical noise resulting from the different schemes used to solve the ordinary differential equations (Runge-Kutta versus Euler schemes). tariq2-plotallvxd [NR]

sixteen rays were ray traced through a VTI model with $v(x,z) = 2 + 0.2x$ km/s, and $\eta(x,z) = 0.1 + 0.05z + 0.05x$. The raytracing was done in the $(x-\tau)$-domain coordinates, and, as a result, the rays and corresponding wavefronts appear in the $(x-\tau)$-domain. The vertical velocity varies considerably between the two sets of curves (black and gray), and yet the two curves coincide exactly. That is because in both models $\alpha$, which is the ratio of the vertical to NMO $P$-wave velocity, does not vary laterally— a condition for the independence of raytracing from vertical velocity in the $(x-\tau)$-domain. Therefore, under this condition, raytracing is dependent on only $v$ and $\eta$.

However, when $\alpha$ varies laterally, raytracing does depend on the vertical velocity. The amount of its dependence is controlled by the size of the lateral variation in $\alpha$. Figure 3 shows rays penetrating in the same model as Figure 2, but with the gray curves corresponding to a laterally varying $\alpha$ that satisfies

$$\alpha(x,z) = \frac{(1.5+0.1x)(1+0.5z)}{2+0.2x}.$$

On the other hand, for the black curves, $\alpha = 0.75$. For the laterally varying $\alpha$ model, at $x = 0$ and $z = 5$ km, $\alpha$=2.625, while at $x = 5$ and $z = 5$ km, $\alpha$=2.333. This big difference corresponds to a large variation in the ratio of the vertical to NMO $P$-wave velocity, a lot more than would be expected in practice. Yet the differences in traveltimes between the two models is moderate. This fact implies that, despite the apparent influence of vertical velocity on raytracing in the $(x-\tau)$-domain coordinates, when $\alpha$ varies laterally, such influence is overall small.

Considering that $\delta$, the parameter that relates the vertical and NMO velocity, ranges typically between -0.1 and 0.4 [3], Figure 4 shows a more practical $\alpha$ variation, in which the curves given by the two models are extremely close. The slightness of the variation suggests that for practical applications of the $(x-\tau)$-domain coordinate processing, we can simply ignore the vertical velocity, and rely on the NMO velocity and $\eta$.

## A LENS EXAMPLE

The presence of a lens anomaly in a velocity model results in a variety of ray paths, the most interesting of which is a development of a triplication in the wavefront. This multi-arrival traveltime phenomenon typically occurs when a negative velocity anomaly is present. The intriguing issue is that triplication can also occur when we have positive $\eta$ anomalies.

Figure 5 shows rays and corresponding wavefronts that were obtained using conventional raytracing in the depth domain (black curves), and using the equivalent raytracing in the $(x-\tau)$-domain (gray curves) through a VTI model with $\eta$=0.1.

[3] this is a wide range; some studies have $\delta$ at a narrower range

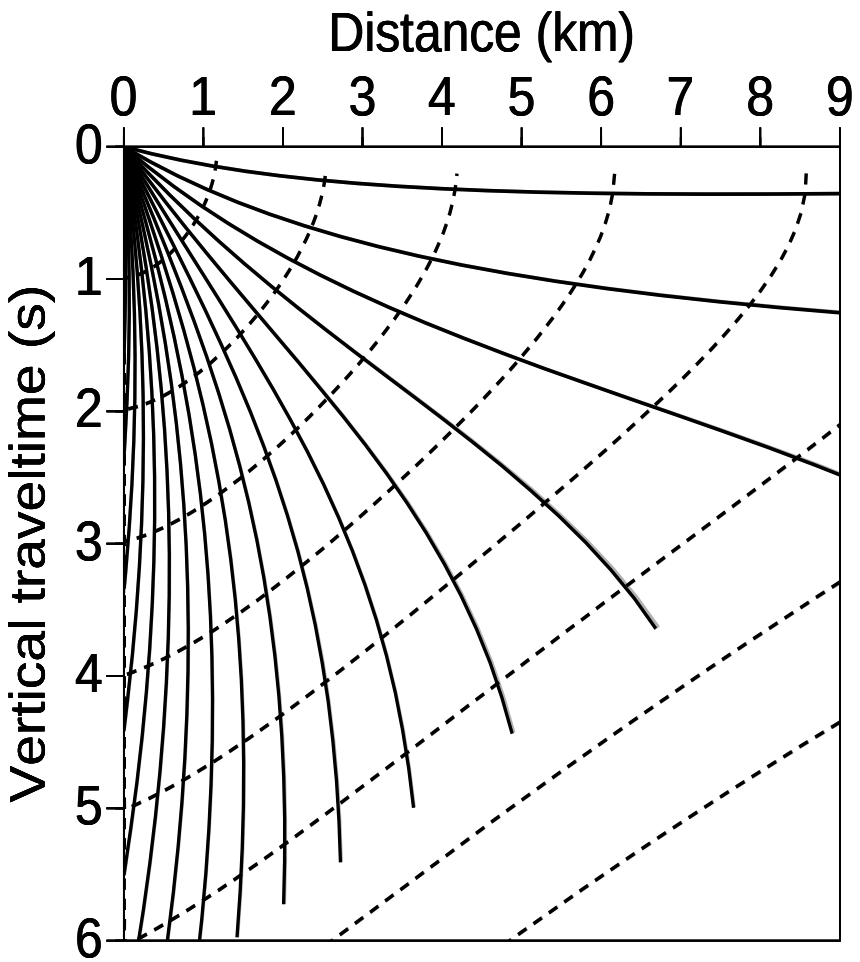


Figure 2: Raypaths and corresponding wavefronts in the $(x-\tau)$-domain for an inhomogeneous VTI model with $v(x,z) = 2+0.2x$ km/s, and $\eta(x,z) = 0.1+0.05z+0.05x$. The black curves correspond to $v_v(x,z) = 1.5 + 0.15x$ km/s ($\alpha = 0.75$), and the gray curves correspond to $v_v(x,z) = 1.5 + 0.15x + 0.75z + 0.075xz$ km/s ($\alpha(z) = 0.75 + 0.375z$). In both cases, $\alpha$ is laterally invariant, and as a result the two curves overlap. tariq2-plotallvxt [NR]

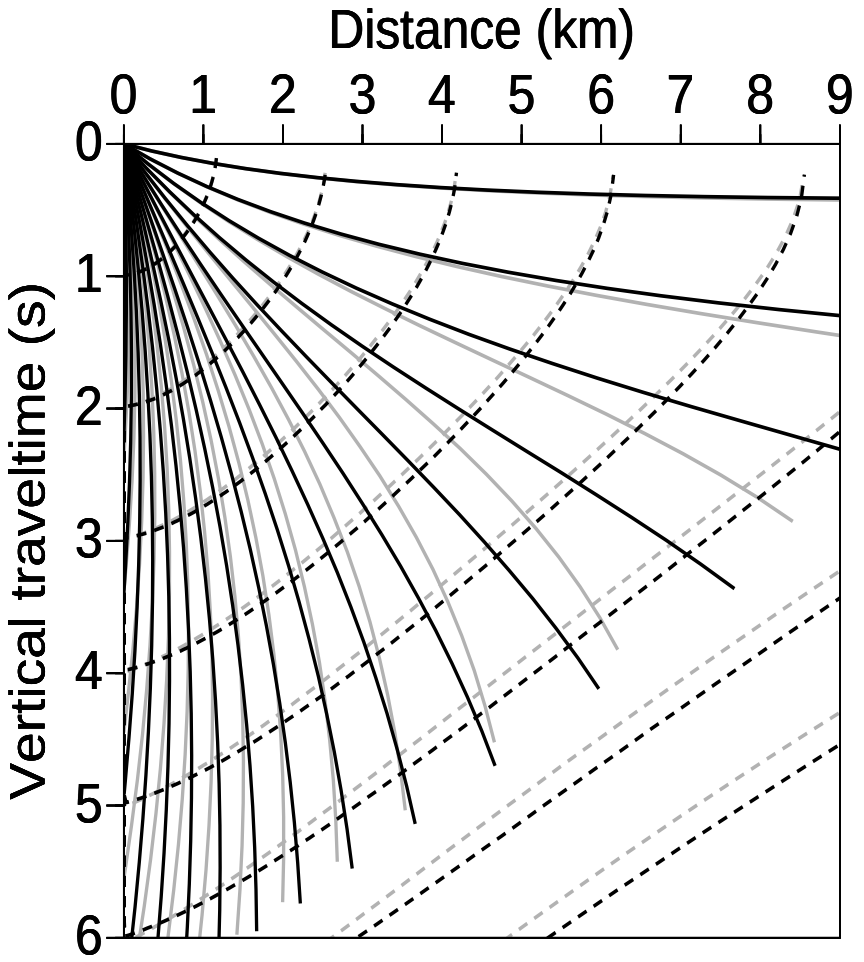


Figure 3: Raypaths and corresponding wavefronts in the $(x-\tau)$-domain for an inhomogeneous VTI model with $v(x,z) = 2+0.2x$ km/s, and $\eta(x,z) = 0.1+0.05z+0.05x$. The black curves correspond to $v_v(x,z) = 1.5 + 0.15x$ km/s ($\alpha = 0.75$), and the gray curves correspond to $v_v(x,z) = 1.5 + 0.1x + 0.75z + 0.05xz$ km/s ($\alpha(x,z) = \frac{(1.5+0.1x)(1+0.5z)}{2+0.2x}$). While for the black curves $\alpha$ is laterally invariant, for the gray curves $\alpha$ varies laterally, and as a result, the black and gray curves no longer coincide. tariq2-plotallvxterr [NR]

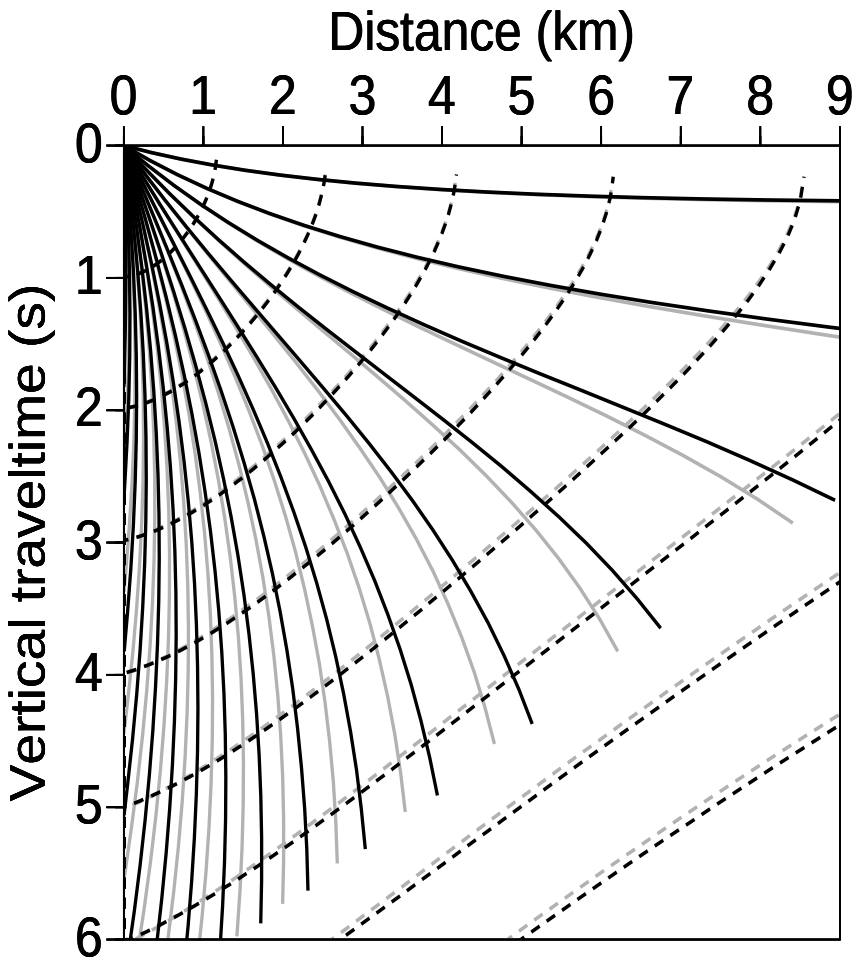


Figure 4: Raypaths and corresponding wavefronts in the $(x-\tau)$-domain for an inhomogeneous VTI model with $v(x,z) = 2+0.2x$ km/s, and $\eta(x,z) = 0.1+0.05z+0.05x$. The black curves correspond to $v_v(x,z) = 1.5 + 0.15x$ km/s ($\alpha = 0.75$), and the gray curves correspond to $v_v(x,z) = 1.5 + 0.13x + 0.75z + 0.065xz$ km/s ($\alpha(x,z) = \frac{(1.5+0.13x)(1+0.5z)}{2+0.2x}$). Despite the fact that for the gray curves $\alpha$ varies laterally, the two curves are extremely close. tariq2-plotallvxterr2 [NR]

The velocity model is shown in the background with a negative velocity anomaly that has a peak of -1.0 km/s. The result is a noticeable triplication that develops soon after the rays pass the anomaly. Despite the triplication, the results of raytracing in the two domains (depth and time) are similar.

Figure 6 also shows raypaths through an anomaly. The anomaly now is in $\eta$, and it is positive. Therefore, the background is an $\eta$ model, with $\eta$=0 everywhere other than in the anomaly. Again, the black curves correspond to solutions of raytracing in the depth domain, while the gray curves correspond to raytracing in the $(x-\tau)$-domain. Triplication, smaller than that associated with the velocity perturbation, occurs in the wavefront. Velocity-wise this medium is homogeneous; it is $\eta$ that is causing the severe bending of the rays! The rays with larger propagation angles from the vertical are the most influenced by the $\eta$ anomaly.

## FINITE-DIFFERENCE SOLUTIONS OF THE $X-TAU$ WAVE EQUATION

In a general inhomogeneous medium, finite difference is the most practical method for solving the wave equation. Despite its enormous computational cost, finite-difference schemes provide a comprehensive solution of the wave equation, which includes an accurate representation of amplitude.

In this example, we use the second-order acoustic wave equation for VTI media in $(x-\tau)$-domain, given by equation (27) and therefore need to solve simultaneously

$$\frac{\partial^2 P}{\partial t^2} = -8\,\frac{\partial^4 F}{\partial x^2 \partial \tau^2}\,v^2\,\eta + \frac{\partial^2 P}{\partial x^2}\,v^2\,(1+2\,\eta) - 16\,\frac{\partial^4 F}{\partial x \partial \tau^3}\,v^2\,\eta\,\sigma + 2\,\frac{\partial^2 P}{\partial x \partial \tau}\,v^2\,(1+2\,\eta)\,\sigma$$
$$-8\,\frac{\partial^4 F}{\partial \tau^4}\,v^2\,\eta\,\sigma^2 + \frac{\partial^2 P}{\partial \tau^2}\,\left(4 + v^2\,(1+2\,\eta)\,\sigma^2\right) + f, \quad (28)$$

and

$$P = \frac{\partial^2 F}{\partial t^2},$$

where $f(x,\tau)$ is the forcing function. We use a second-order finite-difference approximation for $P$-derivatives in equation (28) and a fourth-order approximation for $F$-derivatives. The solution for elliptically anisotropic media is obtained by setting $\eta$=0. Since Alkhalifah (1997d) discusses in detail finite-difference application to a fourth-order equation closely resembling this one, no detailed discussion is included here.

Figure 7 shows a velocity model in depth (on the top), and its equivalent mapping in time (bottom). Figure 8 shows the wavefield at 0.65 s resulting a source igniting at time 0 s, that corresponds to the isotropic velocity model in Figure 7. The wavefield is computed using finite-difference approximations of equation (26). The velocity model given in the $(x-\tau)$-domain is the input velocity model in the finite-difference application. This same velocity model is used to map the wavefield solution back to

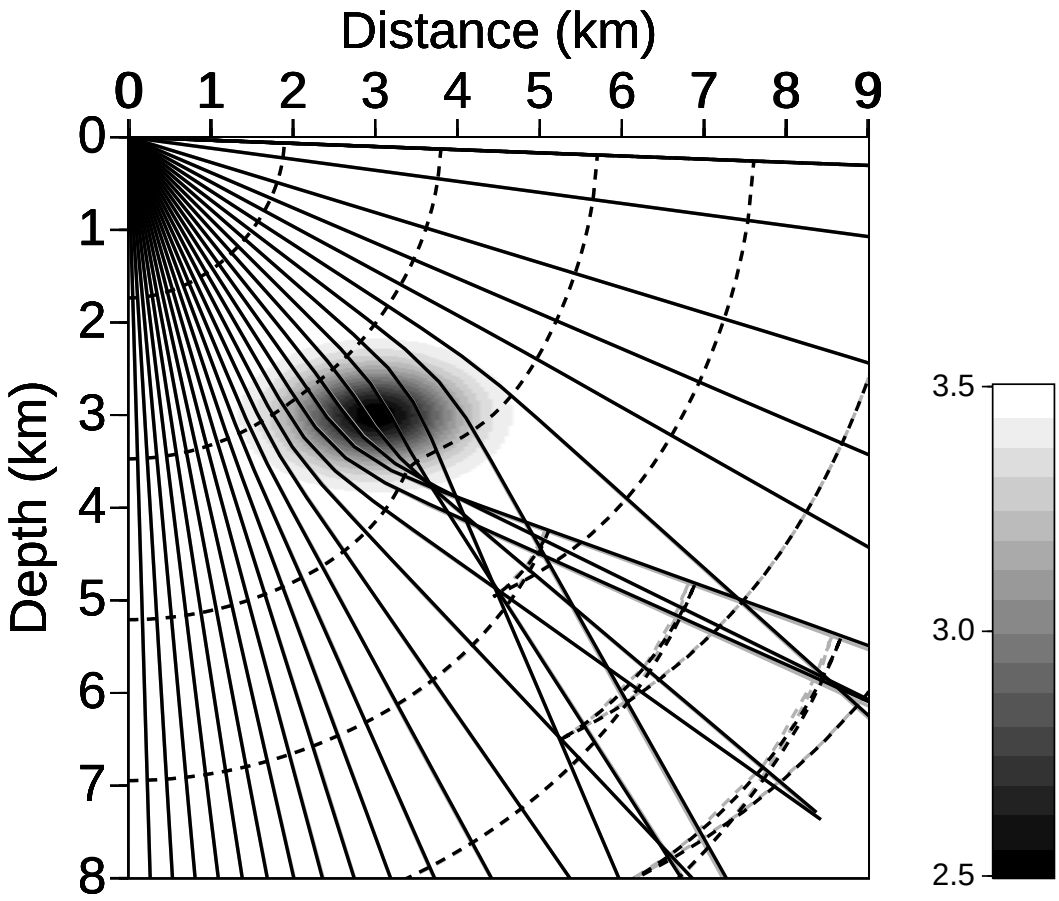


Figure 5: Raypaths (solid curves) and corresponding wavefronts (dashed curves) for an inhomogeneous VTI model, with $\eta = 0.1$. The rays are superimposed on the velocity model, given in km/s, of a negative velocity anomaly. The black curves are obtained through conventional raytracing in the depth domain, and the gray curves are obtained using the equivalent $(x-\tau)$-domain raytracing, where the results are later converted to depth. The curves nearly overlap even in the presence of triplication. tariq2-plotvlensf [NR]

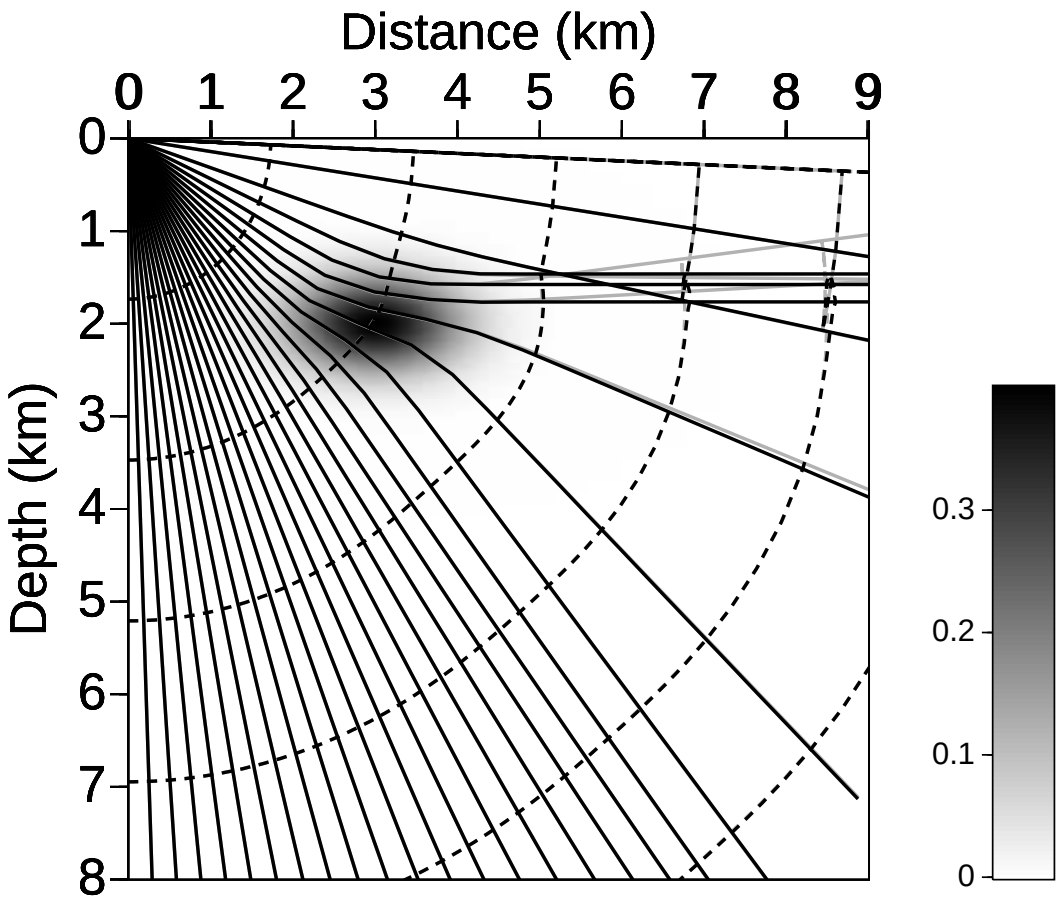


Figure 6: Raypaths and wavefronts for an inhomogeneous VTI model, with $v = 3.5$ km/s. The rays are superimposed on the $\eta$ distribution, which includes a positive $\eta$ anomaly. The black curves are obtained through conventional raytracing in the depth domain, and the gray curves are obtained using the equivalent $(x - \tau)$-domain raytracing, where the results are later converted to depth. The curves nearly overlap even in the presence of $\eta$-induced triplication. tariq2-plotetalensf [NR]

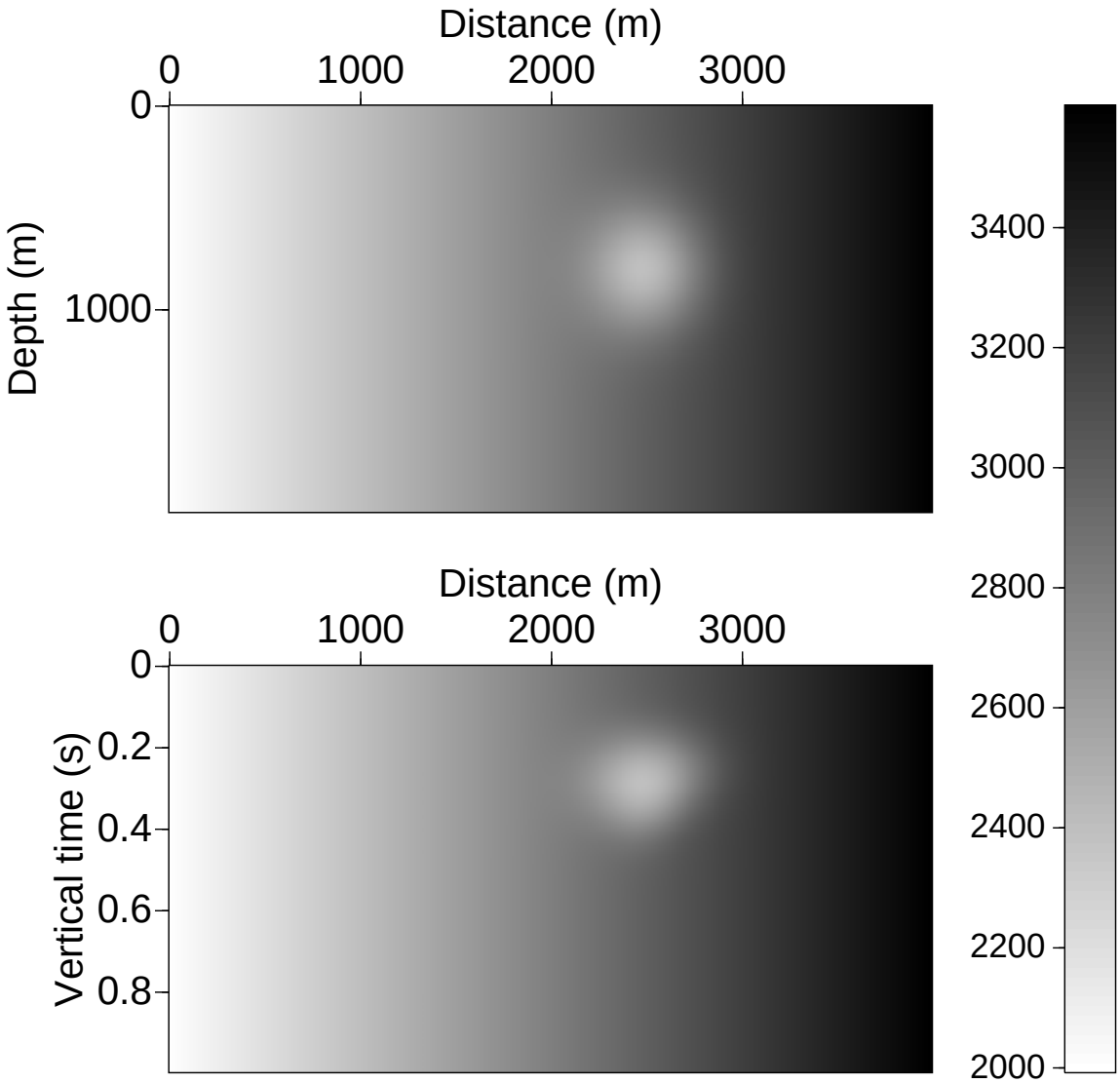


Figure 7: Velocity models in the conventional depth domain (top), and in the $(x-\tau)$-domain (bottom). The velocity model includes a negative velocity anomaly perturbed from a background medium with $v(x) = 2000 + 0.4x$ m/s. tariq2-velwave [NR]

depth. The solid curves in Figure 8 show the solution of the conventional eikonal solver (Vidale, 1990) implemented in the depth domain, and these curves nicely envelope the wavefield solution. Therefore, computing the wavefield in the $(x-\tau)$-domain and in the conventional depth domain are equivalent, regardless of the lateral inhomogeneity. However, the $(x-\tau)$-domain implementation becomes independent of vertical $P$-wave velocity when $\frac{d\alpha}{dx}=0$. Is is also important to note that the apparent frequency of the time section is velocity independent, while waves in the depth section have wavelengths very much dependent on velocity.

## CONCLUSIONS

We derived an eikonal equation that describes the kinematics of wave propagation in the time-domain. This eikonal equation provides exact traveltimes for a general inhomogeneous VTI, or isotropic, media. One of its main features is its independence from the vertical $P$-wave velocity in VTI media, assuming that the ratio of the vertical-to-NMO velocity in VTI media is laterally homogeneous, or in other words, that the anisotropy parameter $\delta$ does not change laterally. Even if $\delta$ varies laterally, the impact of the variation on traveltimes is generally small. As a result, for practical purposes, traveltime calculation in this new $(x-\tau)$-domain is dependent on two parameters in VTI media, and one in elliptically anisotropic media. Using the eikonal equation, we derive an acoustic wave equation that describes wave propagation in the $(x-\tau)$ domain. The existence of this wave equation implies that the amplitudes are also accurately calculated in the $(x-\tau)$-domain. In summary, this paper establishes the basis for a full inhomogeneous time-processing scheme in VTI media that is dependent on only $v$ and $\eta$, and independent of the vertical $P$-wave velocity.

## REFERENCES

Alkhalifah, T., and Tsvankin, I., 1995, Velocity analysis for transversely isotropic media: Geophysics, **60**, 1550–1566.

Alkhalifah, T., 1997a, Acoustic approximations for seismic processing in transversely isotropic media: accepted to Geophysics.

Alkhalifah, T., 1997b, An acoustic wave equation for anisotropic media: This issue of the SEP report.

Biondo, B. V., Fomel, S., and Alkhalifah, T. A., 1997, Focussing eikonal????: SEP-95.

Hatton, L., Larner, K. L., and Gibson, B. S., 1981, Migration of seismic data from inhomogeneous media: Geophysics, **46**, no. 5, 751–767.

Shearer, P. M., and Chapman, C. H., 1988, Ray tracing in anisotropic media with linear velocity gradient: Geophys.J. Int., **94**, no. 5, 575–580.

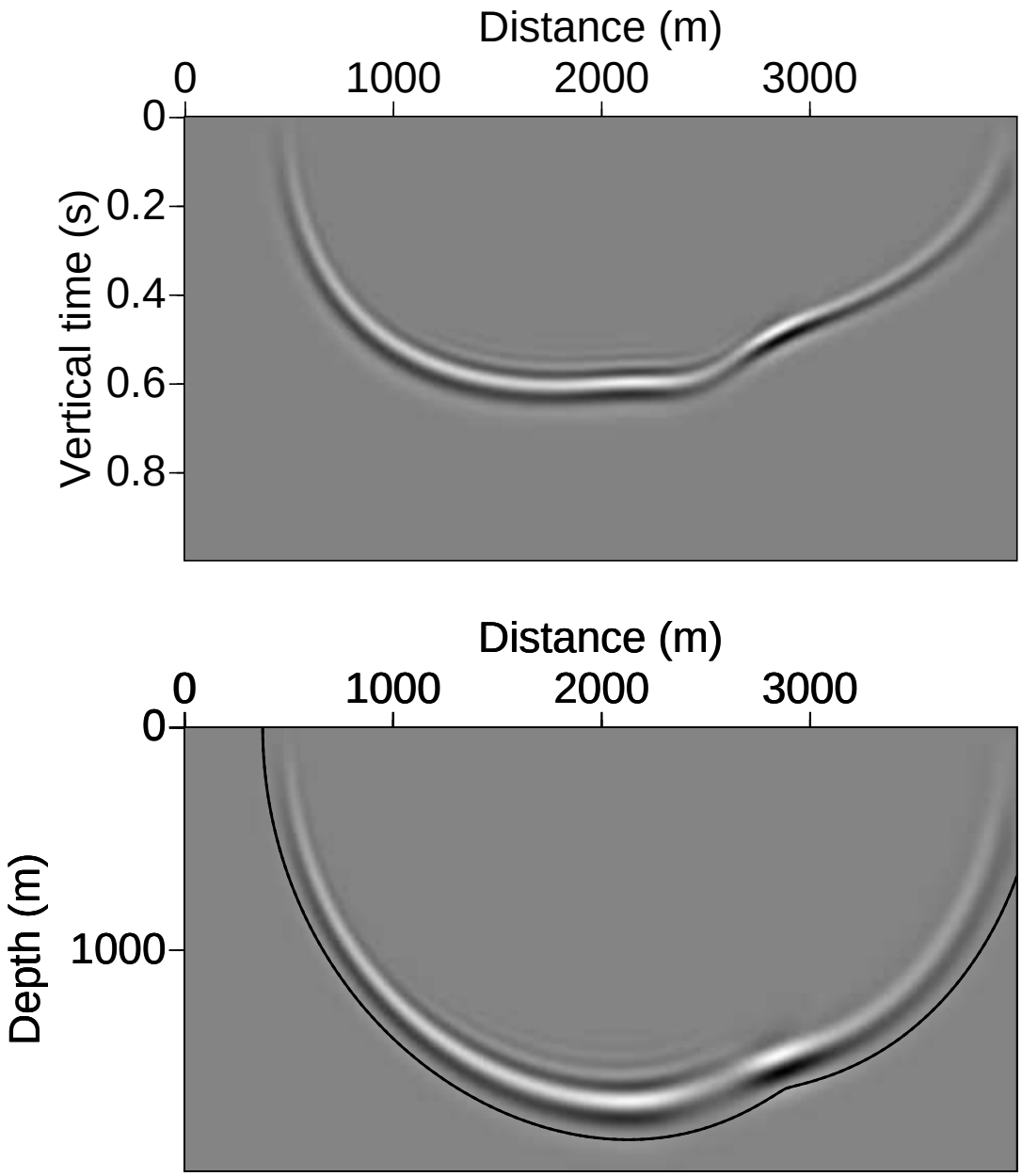


Figure 8: Top: The wavefield in the $(x-\tau)$-domain at 0.65 s resulting from a source at distance 2000 m and $\tau$=0 for the isotropic velocity model shown in Figure 7. Bottom: the same wavefield solution after mapping back to depth using the same velocity model. The black curve is the solution of the eikonal equation for the velocity model in Figure 7 implemented using the conventional depth-domain eikonal solver. tariq2-wavepr [NR]

Thomsen, L., 1986, Weak elastic anisotropy: Geophysics, **51**, no. 10, 1954–1966.

Tsvankin, I., and Thomsen, L., 1994, Nonhyperbolic reflection moveout in anisotropic media: Geophysics, **59**, no. 8, 1290–1304.

Vidale, J. E., 1990, Finite-difference calculation of traveltimes in three dimensions: Geophysics, **55**, no. 5, 521–526.

## APPENDIX A

## THE STRETCH FACTOR IN TIME

In this appendix, we derive $\sigma$, given by equation 6, in the $(x-\tau)$-domain. Using such an equation can avoid the process of mapping $\sigma$ from depth to time and back. The vertical two-way traveltime, $\tau$, is written as

$$\tau(x,z) = \int_0^z \frac{2}{v_v(x,\zeta)} d\zeta, \tag{D-1}$$

where $z$ corresponds to depth. Similarly,

$$z(\tilde{x},\tau) = \frac{1}{2}\int_0^\tau v_v(\tilde{x},t)dt, \tag{D-2}$$

where $\tilde{x}$ corresponds to the new coordinate system.

Using the chain rule,

$$\frac{\partial t}{\partial \tilde{x}} = \frac{\partial t}{\partial x} + \frac{\partial t}{\partial z}\beta, \tag{D-3}$$

where $\beta$ extracted from equation (D-2) is given by

$$\beta(\tilde{x},\tau) = \frac{\partial z}{\partial \tilde{x}} = \frac{1}{2}\int_0^\tau \frac{\partial v_v(\tilde{x},t)}{\partial \tilde{x}}\, dt, \tag{D-4}$$

the partial derivative in $\tau$ is

$$\frac{\partial t}{\partial \tau} = \frac{v_v}{2}\frac{\partial t}{\partial z}. \tag{D-5}$$

Therefore, the transformation from $(\tilde{x},\ \tau)$ to $(x,\ z)$ is governed by the following Jacobian matrix in 2-D:

$$J_c = \begin{pmatrix} 1 & \beta \\ 0 & \frac{v_v}{2} \end{pmatrix}. \tag{D-6}$$

The inverse of $J_c$ is

$$J_c^{-1} = \begin{pmatrix} 1 & \frac{-2\,\beta}{v_v} \\ 0 & \frac{2}{v_v} \end{pmatrix}, \tag{D-7}$$

which should equal the Jacobian matrix for the transformation from $(x,\, z)$ to $(\tilde{x},\, \tau)$, given by

$$J = \begin{pmatrix} 1 & \sigma \\ 0 & \frac{2}{v_v} \end{pmatrix}. \tag{D-8}$$

As a result,

$$\sigma(\tilde{x}, \tau) = \frac{-2\,\beta}{v_v} = \frac{-1}{v_v(\tilde{x}, \tau)} \int_0^\tau \frac{\partial v_v(\tilde{x}, t)}{\partial \tilde{x}}\, dt,$$

which is a convenient equation, since we want to keep all fields, including velocity, in $\tilde{x} - \tau$ coordinates.

## APPENDIX B

## THE AMPLITUDE TRANSPORT EQUATION

To obtain the transport equation for this new $(x - \tau)$-domain coordinate system, we use a ray-theoretical model of the image,

$$F(x, \tau, t) = A(x, \tau) f[t - \tilde{t}(x, \tau)],$$

as a trial solution to the wave equation (23). This procedure yields the eikonal equation as well as the transport equation that describes amplitude behavior, $A(x, y, z)$, of wave propagation. Substituting the trial solution into the partial differential equation (23) and considering only the terms with the highest asymptotic order (those containing the fourth-order derivative of $F$) yields the eikonal equation (9). The next asymptotic order (third-order in derivatives of $F$) gives us a linear partial differential equation of the amplitude transport, as follows:

$$\begin{aligned} 2\,v^2\,A_x\,\left(\tilde{t}_x + \sigma\,\tilde{t}_\tau\right)\left(1 + 2\,\eta - 8\,\eta\,\tilde{t}_\tau^2\right) + A\left(v^2\,(1 \;+\; 2\,\eta)\,\sigma^2 - 8\,v^2\,\eta\,\left(\tilde{t}_x^2 + 6\,\sigma\,\tilde{t}_x\,\tilde{t}_\tau + 6\,\sigma^2\,\tilde{t}_\tau^2\right)\tilde{t}_{\tau\tau}\right) + \\ 2\,A_\tau\,\left(-8\,v^2\,\eta\,\tilde{t}_x^2\,\tilde{t}_\tau + v^2\,\sigma\,\tilde{t}_x\,\left(1 + 2\,\eta - 24\,\eta\,\tilde{t}_\tau^2\right) \;+\; \tilde{t}_\tau\,\left(4 + v^2\,(1 + 2\,\eta)\,\sigma^2 - 16\,v^2\,\eta\,\sigma^2\,\tilde{t}_\tau^2\right)\right) + \\ 4A + Av^2\left(2\,\left(\sigma + 2\,\eta\,\sigma - 8\,\eta\,\tilde{t}_\tau\,\left(2\,\tilde{t}_x + 3\,\sigma\,\tilde{t}_\tau\right)\right)\tilde{t}_{x\tau} \;+\; \left(1 + 2\,\eta - 8\,\eta\,\tilde{t}_\tau^2\right)\tilde{t}_{xx}\right) = 0. \end{aligned} \tag{B-1}$$

Setting $\eta = 0$, yields the corresponding transport equation for elliptically anisotropic media,

$$\begin{aligned} 2\,v^2\,A_x\,\left(\tilde{t}_x + \sigma\,\tilde{t}_\tau\right) + 2\,A_\tau\,\left(v^2\,\sigma\,\tilde{t}_x + \left(4 + v^2\,\sigma^2\right)\,\tilde{t}_\tau\right) + \\ A\,\left(v^2\,\left(\tilde{t}_{xx} + 2\,\sigma\,\tilde{t}_{x\tau}\right) + \left(4 + v^2\,\sigma^2\right)\,\tilde{t}_{\tau\tau}\right) = 0. \end{aligned} \tag{B-2}$$

Both transport equations include first-and second-order derivatives of time with respect to position, calculated from the solution of the eikonal equation. Despite the apparent complexity of the transport equations, they are linear, and contain only first-order derivates of $A$. As expected, amplitudes depend on second-order derivatives of traveltime, or wavefront curvature. The dynamic raytracing equations behave

similarly. Also, we can see that equations (B-1) and (B-2) include terms corresponding to cross derivates of traveltime (i.e., $\frac{\partial^2 t}{\partial x \partial \tau}$), which result from the cross-dependent nature of the new coordinate system. Some of these terms are caused by anisotropy (Alkhalifah, 1997d). When $\sigma = 0$ in equation (B-2) all such cross-derivate terms drop out.